ELSEVIER

Colloids and Surfaces B: Biointerfaces 13 (1999) 277–286

COLLOIDS AND SURFACES B

Effect of pH on the electrophoretic mobility of a particle with a charge-regulated membrane in a general electrolyte solution

Shiojenn Tseng [a,*], Sung-Hwa Lin [b], Jyh-Ping Hsu [b]

[a] *Department of Mathematics, Tamkang University, Tamsui, Taipei 25173, Taiwan, ROC*
[b] *Department of Chemical Engineering, National Taiwan University, Taipei 10617, Taiwan, ROC*

Received 15 March 1999; accepted 08 April 1999

Abstract

The electrophoretic motion of an entity comprised of a rigid, uncharged core covered by a charge-regulated membrane which simulates a biological cell, in a general a:b electrolyte solution is analyzed. The membrane carries a fixed charge which arises from the dissociation of the acidic functional group HA. We show that the higher the concentration of cations in the bulk liquid phase, the lower the absolute Donnan potential, $|\varphi_D|$, and the lower the concentration of functional group, N_0, the lower the $|\varphi_D|$. Also, the higher the pH, the higher the absolute electrical potential, and the greater the N_0, the lower the pH. The absolute mobility of a cell, $|\mu|$, increases with pH, but decreases with the increase in the friction coefficient of the membrane phase, γ. For a fixed total number of HA, if γ is large, μ/μ_s is less than unity, μ_s being the mobility of the corresponding rigid particle, and it decreases with the thickness of membrane d, and the inverse is true if γ is small. For a medium γ, the variation of μ/μ_s as a function of d has a local maximum, and depending upon d, it can be either greater or less than unity.

Keywords: Electrophoretic mobility; Charge-regulated membrane; Dissociable acidic function groups; General electrolyte; Donnan potential

1. Introduction

The electrophoretic behavior of a biological cell in an applied electric field provides important information about its properties such as the sign of surface charge and the level of surface potential. For a rigid spherical particle, if the electrical double layer is thin, it can be shown that the following relation holds [1]:

$$\mu_s = U/E = \varepsilon\zeta/\eta, \tag{1}$$

where μ_s and U denote respectively the electrophoretic mobility and the velocity of the particle, E and ζ are respectively the strength of applied electric field and the zeta potential, and ε

* Corresponding author. Fax: +886-2-6202613.
E-mail address: tseng@math.tku.edu.tw (S. Tseng)

0927-7765/99/$ - see front matter
PII: S0927-7765(99)00040-5

and η the permittivity and the viscosity of the liquid phase, respectively.

A biological cell can be simulated by a rigid, uncharged core coated by a membrane layer, which is ion-penetrable and carries dissociable functional groups [2–5]. Human erythrocytes, for example, have a glycoprotein layer of ~ 15 nm thick which forms the outer boundary of the lipid layer [6,7]. In this case, since the fixed charges carried by a particle are distributed in the membrane layer, rather than over a rigid surface, Eq. (1) needs to be modified accordingly.

It is often assumed that the electrical potential is low and the liquid phase contains symmetric electrolytes. This is mainly because that solving analytically the Poisson–Boltzmann equation, which governs the spatial variation of the electrical potential of the system under consideration, is almost impossible in the general case. Ohshima and Kondo [8] solved the problem of a planar particle covered by a charged ion-penetrable surface layer in a symmetric electrolyte solution. The problem of an ion-penetrable spherical particle in a general electrolyte solution was discussed by Ohshima [9]. In these studies, the difficulty of solving a nonlinear Poisson–Boltzmann equation prohibits the derivation of an explicit expression for both electrical potential and the mobility of a particle. Ohshima et al. [10,11] examined the electrophoretic mobility of a planar colloidal particle covered by an ion-penetrable surface layer having uniformly distributed fixed charge. A more general case in which the fixed charge can assume a linear or exponential distribution was discussed by Hsu et al. [12]. Ohshima et al. [13] considered the case of an arbitrary non-uniform fixed-charge distribution. Hsu et al. [14] investigated the electrophoretic mobility of an ion-penetrable cell having an arbitrary continuous fixed-charge distribution. A 1:1 electrolyte solution was assumed, and the governing equations were solved numerically. Hsu and Fan [15] modeled the electrophoretic mobility of a planar particle coated with an ion-penetrable charged membrane in a uniform electric field taking the effects of the distributions of fixed charge and dielectric constant into account. In an analysis of the electrophoretic mobility of a planar particle covered by an ion-penetrable membrane in an asymmetric electrolyte solution Hsu et al. [16] were able to derive a semi-analytical result for the case of uniformly distributed fixed charge.

Here, we consider the problem in which the degree of dissociation of the functional groups in the membrane, and, therefore, the distribution of fixed charge carried by a particle, is dependent upon the conditions of the liquid phase. This extends the analysis of Hsu et al. [16] to a more general case. In particular, we will focus on the effect of pH on the electrophoretic mobility of a cell.

2. Modeling

By referring to Fig. 1, we consider a particle comprises a rigid, uncharged core and an ion-penetrable membrane of thickness d. The particle is immersed in an arbitrary a:b electrolyte solution, and an electric field E parallel to its surface with strength E is applied. The membrane contains uniformly distributed functional group HA, which is capable of undergoing the dissociation reaction

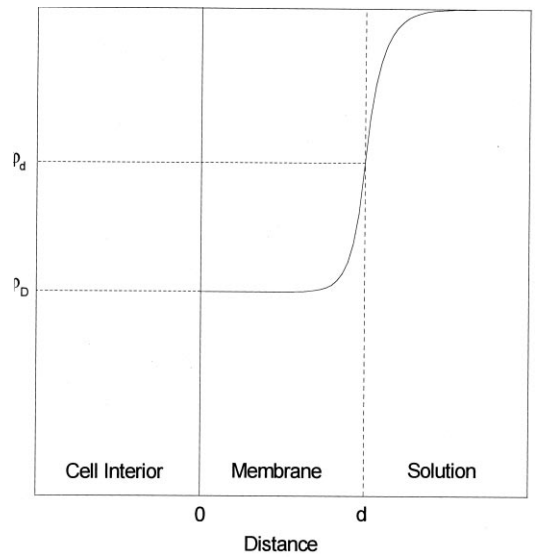

Fig. 1. A schematic representation of the system under consideration where d is the thickness of membrane, ϕ_d denotes the electrical potential at the membrane–solution interface, and ϕ_D represents the Donnan potential.

$$HA = H^+ + A^- \quad (2)$$

This expression implies that the fixed charge in the membrane phase is negative, and the particle migrates in the direction opposite to E. In practice, since the linear size of a cell is much larger than the thickness of the electrical double layer near cell surface, the cell surface can be considered as planar, and a one-dimensional description is satisfactory.

2.1. Distribution of electric potential

If the dielectric constant of the liquid phase ε is constant, the spatial variation of electric potential φ can be described by the Poisson equation [1]

$$\nabla^2\varphi = -\frac{\rho}{\varepsilon}, \quad (3)$$

where ρ denotes the space charge density. Suppose that the pH of the bulk solution is constant, and both the dissociation reaction represented by Eq. (2) and the distributions of ions in the liquid phase are at equilibrium. Then, we have

$$[H^+(x)] = C_H^0 \exp\left[-\frac{F\varphi(x)}{RT}\right], \quad (4a)$$

$$K_e = \frac{[H^+(x)]\,[A^-(x)]}{[HA(x)]}, \quad (4b)$$

where K_e denotes the equilibrium constant for the dissociation reaction expressed in Eq. (2), F and R are the Faraday and gas constant, respectively, T is the absolute temperature, x denotes the position variable, and $[H^+]$, $[A^-]$, and [HA] represent respectively the concentrations of H^+, A^-, and HA. The value of $[A^-]$ can be determined from Eqs. (4a) and (4b), and the conservation of [HA] as

$$[A^-(x)] = \frac{N_0}{[1 + C_H^0 \exp(-F\varphi(x)/RT)/K_e]}, \quad (4c)$$

where C_H^0 and N_0 are, respectively, the bulk concentration of H^+ and the concentration of the functional group. The spatial variation of the fixed charge in the membrane phase $\rho_{fix}(x)$ can be expressed as

$$\rho_{fix}(x) = -F[A^-(x)] = -\frac{FN_0}{[1 + C_H^0 \exp(-F\varphi(x)/RT)/K_e]}, \quad (5)$$

In the liquid phase, ρ comprises free ions only, and in the membrane phase it contains both the free ions and ρ_{fix}. Therefore,

$$\rho(x) = aC_a^0F\exp(-aF\varphi/RT) - bC_b^0F\exp(bF\varphi/RT) + C_H^0F\exp(-F\varphi/RT), \quad d \le x < \infty \quad (6a)$$

$$\rho(x) = aC_a^0F\exp(-aF\varphi/RT) - bC_b^0F\exp(bF\varphi/RT) + C_H^0F\exp(-F\varphi/RT) - N_0F/[1 + C_H^0\exp(-F\varphi/RT)/K_e], \quad 0 < x < d, \quad (6b)$$

where C_a^0 and C_b^0 are the concentrations of cations and anions, respectively. Substituting Eqs. (6a) and (6b) into Eq. (3), and employing the electroneutrality condition

$$aC_a^0 - bC_b^0 + C_H^0 = 0, \quad (7)$$

we obtain

$$\varepsilon_1\frac{d^2\varphi}{dx^2} = aC_a^0F[\exp(bF\varphi/RT) - \exp(-aF\varphi/RT)] + C_H^0F[\exp(bF\varphi/RT) - \exp(-F\varphi/RT) + N_0F/[1 + C_H^0\exp(-F\varphi/RT)/K_e], \quad 0 < x < d \quad (8a)$$

$$\varepsilon_2\frac{d^2\varphi}{dx^2} = aC_a^0F[\exp(bF\varphi/RT) - \exp(-aF\varphi/RT)] + C_H^0F[\exp(bF\varphi/RT) - \exp(-F\varphi/RT) \quad d \le x < \infty \quad (8b)$$

In these expressions, ε_1 and ε_2 denote respectively the permittivity of the membrane phase and that of the liquid phase. The boundary conditions associated with Eqs. (8a) and (8b) are assumed to be

$$\varphi \to 0 \text{ and } d\varphi/dx \to 0 \quad \text{as} \quad x \to \infty \quad (9a)$$

$$\varphi(x \to d^-) = \varphi(x \to d^+) = \varphi_d \quad (9b)$$

$$\varepsilon_1(\mathrm{d}\varphi/\mathrm{d}x)_{x\to d^-} = \varepsilon_2(\mathrm{d}\varphi/\mathrm{d}x)_{x\to d^+} \tag{9c}$$

$$\mathrm{d}\varphi/\mathrm{d}x = \mathrm{d}^2\varphi/\mathrm{d}x^2 = 0 \quad \text{and} \quad \varphi = \varphi_\mathrm{D} \quad \text{as} \quad x\to 0, \tag{9d}$$

The last expression arises from the condition that the membrane is thick compared with double layer, and the potential at the inner side of the membrane reaches an asymptotic value φ_D, the Donnan potential [17]. For a simpler treatment, Eqs. (8a) and (9d) are rewritten in the following scaled forms:

$$\frac{\mathrm{d}^2\psi}{\mathrm{d}X^2} = \varepsilon'[aG_1 + M_\mathrm{H}G_2 + M_0G_3], \qquad 0 < X < d' \tag{10a}$$

$$\frac{\mathrm{d}^2\psi}{\mathrm{d}X^2} = aG_1 + M_\mathrm{H}G_2, \qquad d' \le X < \infty \tag{10b}$$

$$\psi\to 0 \quad \text{and} \quad \mathrm{d}\psi/\mathrm{d}X\to 0 \quad \text{as} \quad X\to\infty \tag{11a}$$

$$\psi(X\to d'^-) = \psi(X\to d'^+) = \psi_d \tag{11b}$$

$$(\mathrm{d}\psi/\mathrm{d}X)_{X\to d'^-} = \varepsilon'(\mathrm{d}\psi/\mathrm{d}X)_{X\to d'^+} \tag{11c}$$

$$\mathrm{d}\psi/\mathrm{d}X = \mathrm{d}^2\psi/\mathrm{d}X^2 = 0, \quad \text{and} \quad \psi = \psi_\mathrm{D} \ \text{as} \ X\to\infty \tag{11d}$$

In these expressions, $\psi = F\varphi/RT$, $\varepsilon' = \varepsilon_2/\varepsilon_1$, $X = \kappa_2 x$, $G_1 = \exp(b\psi) - \exp(-a\psi)$, $G_2 = \exp(b\psi) - \exp(-\psi)$, $G_3 = 1/[1 + M_\mathrm{e}\ \exp(-\psi)]$, $d' = \kappa_2 d$, $M_\mathrm{H} = C^0_\mathrm{H}/C^0_\mathrm{a}$, $M_0 = N_0/C^0_\mathrm{a}$, $M_\mathrm{e} = C^0_\mathrm{H}/K_\mathrm{e}$, and $\kappa_2^2 = C^0_\mathrm{a}F^2/\varepsilon_2 RT$, κ_2 being the reciprocal Debye length. Solving Eq. (10b) subject to Eq. (11a), we have

$$\frac{\mathrm{d}\psi}{\mathrm{d}X} = 2^{1/2}\left\{\frac{a}{b}(e^{b\psi}-1) + e^{-a\psi} - 1 + M_\mathrm{H}\left[\frac{1}{b}(e^{b\psi}-1) + e^{-\psi} - 1\right]\right\}^{1/2}, \qquad d' \le X < \infty \tag{12}$$

Similarly, Eqs. (10a), (11b), (11c) and (12) lead to

$$\frac{\mathrm{d}\psi}{\mathrm{d}X} = (2\varepsilon')^{1/2}\left\{\frac{a}{b}(e^{b\psi}-\varepsilon') + e^{-a\psi} - \varepsilon' + M_\mathrm{H}\left[\frac{1}{b}(e^{b\psi}-\varepsilon') + e^{-\psi} - \varepsilon'\right] + M_0[\ln(e^{\psi} + M_\mathrm{e}) - \ln(e^{\psi d} + M_\mathrm{e})] + (\varepsilon' - 1) \times \left[\frac{a}{b}e^{b\psi_d} + e^{-a\psi_d} + M_\mathrm{H}\left(\frac{1}{b}e^{b\psi_d} + e^{-\psi_d}\right)\right]\right\}^{1/2}, \qquad 0 < X < d' \tag{13}$$

Eqs. (12) and (13) can be rewritten as

$$\frac{\mathrm{d}Y}{\mathrm{d}X} = a(f_1)^{1/2}, \qquad 0 < X < d' \tag{14a}$$

$$\frac{\mathrm{d}Y}{\mathrm{d}X} = a(f_2)^{1/2}, \qquad d' \le X < \infty, \tag{14b}$$

In these expressions, $Y = \exp(a\psi/2)$, $k = 2 + 2b/a$, and

$$f_1 = \frac{\varepsilon'}{2}\left\{\frac{2(a+M_\mathrm{H})}{a(k-2)}\,Y^k + Y^2M_0\ln\left(\frac{Y^{2/a} + M_\mathrm{e}}{Y_d^{2/a} + M_\mathrm{e}}\right) + \{(\varepsilon'-1)\frac{2(a+M_\mathrm{H})}{a(k-2)}\,Y_d^{k-2} + Y_d^{-2} + M_\mathrm{H}Y_d^{-2/a}] - \frac{\varepsilon'[ak + M_\mathrm{H}(ak - 2a + 2)]}{a(k-2)}\right\}Y^2 + M_\mathrm{H}Y^{2-2/a} + 1\}, \qquad 0 < X < d' \tag{15a}$$

$$f_2 = \frac{1}{2}\left[\frac{2(a+M_\mathrm{H})}{a(k-2)}\,Y^k - \frac{ak(1+M_\mathrm{H}) - 2aM_\mathrm{H} + 2M_\mathrm{H}}{a(k-2)}\,Y^2 + M_\mathrm{H}Y^{2-2/a} + 1\right], \qquad d' \le X < \infty \tag{15b}$$

Solving Eqs. (14a) and (14b) analytically for Y is nontrivial, and an approximate method is adopted in the following discussion. Suppose that $f_1^{1/2}$ and $f_2^{1/2}$ can be approximated respectively by

$$f_1^{1/2} \cong a_1Y^2 + b_1Y + c_1, \qquad 0 < X < d' \tag{16a}$$

and

$$f_2^{1/2} \cong a_2Y^2 + b_2Y + c_2, \qquad d' \le X < \infty, \tag{16b}$$

where a_i, b_i, and c_i, $i = 1,2$, are constant. Substituting these expressions into Eqs. (14a) and (14b), and integrating the resultant expressions subject to Eq. (11b), we obtain

$$Y_i = \frac{1}{2a_i}\left[\frac{2P_i}{1 - Q_i(X)} - b_i - P_i\right], \qquad R_i \ge 0, \quad i = 1, 2 \tag{17a}$$

$$Y_i = \frac{1}{2a_i}\left\{P_i \tan\left[\frac{aP_i(X-d')}{2} + \tan^{-1}\left(\frac{2a_i Y_d + b_i}{P_i}\right)\right] - b_i\right\}, \qquad R_i < 0, \quad i = 1, 2 \tag{17b}$$

where $R_i = b_i^2 - 4a_i c_i$, $P_i = \sqrt{|R_i|}$, $i = 1, 2$, and

$$Q_i(X) = \exp[aP_i(X-d')]\left[1 - \frac{2P_i}{(2a_i Y_d + b_i + P_i)}\right], \quad i = 1, 2 \tag{18}$$

In these expressions, i is a region index, $i = 1$ denotes the membrane phase, and $i = 2$ represents the liquid phase.

The Donnan potential can be estimated by combining Eqs. (10a) and (11d) to yield

$$(a + M_H)Y_D^{k-2} - aY_D^{-2} - M_H Y_D^{-2/a} + M_0/(1 + M_e Y_D^{-2/a}) = 0, \tag{19}$$

where $Y_D = \exp(a\psi_D/2)$, ψ_D being the scaled Donnan potential. Eqs. (11d) and (13) yield

$$\frac{a}{b}(e^{b\psi_D} - \varepsilon') + e^{-a\psi_D} - \varepsilon' + M_H\left[\frac{1}{b}(e^{b\psi_D} - \varepsilon') + (e^{-\psi_D} - \varepsilon')\right] + M_0[\ln(e^{\psi_D} + M_e) - \ln(e^{\psi_D} + M_e)] + (\varepsilon' - 1)\left[\frac{a}{b}e^{b\psi_d} + e^{-a\psi_d} + M_H\left(\frac{1}{b}e^{b\psi_d} + e^{-\psi_d}\right)\right] = 0 \tag{20}$$

Once ψ_D is calculated by Eq. (19), this expression can be used to evaluate ψ_d, the scaled potential at the membrane–liquid interface.

2.2. Distribution of velocity

For convenience, we let the cell be fixed in space, and the fluid moves parallel to cell surface in the direction of electric field. The spatial variation of fluid velocity is governed by the Navier–Stokes equation [10]

$$\eta\frac{d^2v(x)}{dx^2} - \gamma v(x) + \rho_{el}(x)E = 0, \quad 0 < x < d \tag{21a}$$

$$\eta\frac{d^2v(x)}{dx^2} + \rho_{el}(x)E = 0, \quad d \le x < \infty \tag{21b}$$

where γ is the frictional coefficient of membrane phase. The following boundary conditions are assumed:

$$v \to -U \quad \text{and} \quad dv/dx \to 0 \quad \text{as} \quad x \to \infty \tag{22a}$$

$$v(x \to d^-) = v(x \to d^+) \tag{22b}$$

$$(dv/dx)_{x \to d-} = (dv/dx)_{x \to d+} \tag{22c}$$

$$v(x \to 0) = 0, \tag{22d}$$

where U is constant. Eqs. (8a), (8b), (21a) and (21b) lead to

$$\frac{d^2u}{dX^2} - \lambda^2 u = \frac{M}{\mu}(aG_1 + M_H G_2), \quad 0 < X < d' \tag{23a}$$

$$\frac{d^2u}{dX^2} = \frac{M}{\mu}\left(\frac{d^2\psi}{dX^2}\right), \quad d' \le X < \infty \tag{23b}$$

where $u = v/U$, $\lambda^2 = \gamma/\eta\kappa_2^2$, and $M = \varepsilon_2 RT/\eta F$. The boundary conditions in Eqs. (22a), (22b), (22c) and (22d), can be rewritten as

$$u \to -1 \quad \text{and} \quad du/dX \to 0 \quad \text{as} \quad X \to \infty \tag{24a}$$

$$u(X \to d^-) = u(X \to d^+) \tag{24b}$$

$$(du/dX)_{X \to d'-} = (du/dX)_{X \to d'+} \tag{24c}$$

$$u(X \to 0) = 0 \tag{24d}$$

Solving Eqs. (23a) and (23b) subject to Eqs. (24a) and (24b) gives

$$u(X) = \frac{M}{\mu}\psi(X) - 1, \quad d' \le X < \infty \tag{25a}$$

$$u(X) = Ae^{\lambda X} + Be^{-\lambda X} + \frac{1}{\mu}W(X), \quad 0 < X < d' \tag{25b}$$

In these expressions, $B = -A$, and

$$A = \frac{1}{2\sinh(\lambda d')}\{\frac{1}{\mu}(M\psi_d - W_1) - 1] \tag{26a}$$

$$W(X) = \frac{1}{2\lambda}[e^{\lambda X}\int_0^X e^{-\lambda X}R_2(X)\,dX - e^{-\lambda X}\int_0^X e^{\lambda X}R_2(X)\,dX] \tag{26b}$$

$$W_1 = \frac{1}{2\lambda}[e^{\lambda d'}\int_0^{d'} e^{-\lambda X}R_2(X)\,dX - e^{-\lambda d'}\int_0^{d'} e^{\lambda X}R_2(X)\,dX] \quad (26c)$$

$$R_2(X) = M(aG_1 + M_H G_2) \quad (26d)$$

2.3. Electrophoretic mobility

The electrophoretic mobility of a cell, μ ($= U/E$), can be determined from Eqs. (25a), (25b) and (24c) as

$$\mu = \frac{1}{\lambda}\tanh(\lambda d')[W_2 - M(d\psi/dX)_{X\to d'+}] - W_1 + M\psi_d \quad (27)$$

where

$$W_2 = \frac{1}{2}[e^{\lambda d'}\int_0^{d'} e^{-\lambda X}R_2(X)\,dX + e^{-\lambda d'}\int_0^{d'} e^{\lambda X}R_2(X)\,dX] \quad (27a)$$

Therefore, μ is a function of both the electrical potential at the membrane–liquid interface and the distribution of electrical potential in the membrane phase.

3. Results and discussion

The coefficients a_i and b_i, $i = 1, 2, 3$, in Eqs. (16a) and (16b) are estimated through regression analysis. Fig. 2 shows the typical variations of $f_1^{1/2}$ and $f_2^{1/2}$ as a function of Y; both the exact values and those estimated based on regression analysis are illustrated. This figure suggests that the approximate expressions, Eqs. (16a) and (16b), are reasonably accurate. Table 1 presents the typical deviation of the electrophoretic mobility predicted on the basis of Eqs. (16a) and (16b) from the exact numerical calculation based on Eqs. (15a) and (15b). This table reveals that the performance of the present approximate method is satisfactory.

Fig. 3 presents the variation in the absolute scaled Donnan potential $|\psi_D|$ as a function of C_a^0 at various pH. The simulated spatial variations of

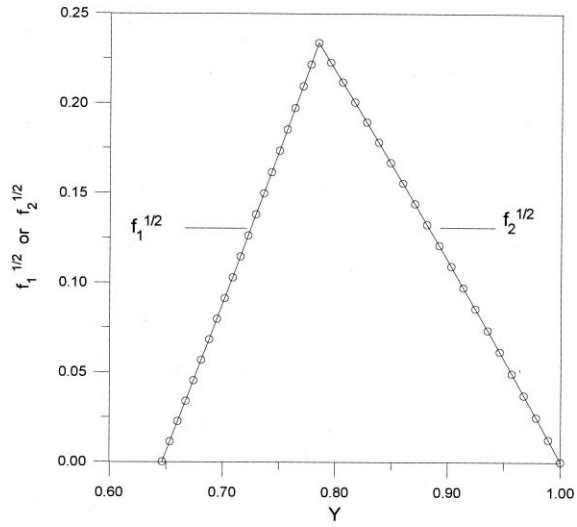

Fig. 2. (a) Variation of $f_1^{1/2}$ as a function of Y; (b) Variation of $f_2^{1/2}$ as a function of Y. The parameters used are $N_0 = 0.05$ M, $C_a^0 = 0.01$ M, $a = 3$ and $b = 1$. The fitted values for the parameters defined in Eqs. (16a) and (16b) are $a_1 = 0.4852$, $b_1 = 1.0023$, $c_1 = -0.8508$, $a_2 = -0.3463$, $b_2 = -0.4644$, and $c_2 = 0.8106$. Solid lines represent the values based on a regression analysis, and open circles the exact values. Key: $\varepsilon' = 1$, $K_e = 1.0 \times 10^{-5}$ M, $C_H^0 = 1.0 \times 10^{-7}$ M, $T = 298.15$ K, and $\varepsilon_2 = 78 \times 8.854 \times 10^{-12}$ C V^{-1}m^{-1}.

the scaled electrical potential ψ at various pH are shown in Fig. 4. Fig. 3 reveals that for a fixed pH, $|\psi_D|$ decreases with the increase in C_a^0. This is because that the higher the C_a^0, the greater the shielding effect of electrolyte, and, therefore, the lower the potential inside the membrane phase. Fig. 3 also shows that for a fixed C_a^0, $|\psi_D|$ increases with pH. According to Eqs. (4b) and (5), the higher the pH, the easier for HA to dissociate, and the higher the concentration of fixed charge, which leads to a higher $|\psi_D|$. This is also justified by Fig. 4.The spatial variation of pH can be derived from Eq. (4a) as

$$\mathrm{pH}(X) = -\log_{10}[H^+(X)] = [\ln(1/C_H^0) - |\psi(X)|]/\ln 10 \quad (28)$$

Fig. 5 shows the spatial variation of pH for various concentrations of the functional group N_0. As can be seen from this figure, pH decreases with the increase in N_0. This is because that the larger the N_0, the higher the absolute potential in

Table 1
Typical percentage deviation (DV) of the electrophoretic mobility based on the approximate expressions (Eqs. (16a) and (16b)), from the exact numerical calculation based on Eq. (13)[a]

a	b	DV
1	1	4.203×10^{-5}
2	1	2.685×10^{-4}
3	1	9.072×10^{-4}
1	2	6.948×10^{-5}
2	2	3.730×10^{-4}
3	2	1.202×10^{-3}
1	3	9.992×10^{-5}
2	3	4.866×10^{-4}
3	3	1.861×10^{-3}

[a] DV = |(approximate-exact)/exact| × 100%. Parameters used are $C_a^0 = 0.01$ M, $C_H^0 = 10^{-7}$ M, $N_0 = 0.01$ M, $K_e = 10^{-5}$ mol m^{-3}, $\varepsilon' = 1$, $z = 1$, $d' = 5$, $\gamma = 10^{12}$ N s m^{-4}.

the membrane phase, and the smaller the pH, as suggested by Eq. (28).

Fig. 6 illustrates the variation in the absolute mobility $|\mu|$ as a function of pH at various values of friction coefficient γ. This figure reveals that for a fixed pH, the larger the γ, the smaller the $|\mu|$, as expected. For a fixed γ, $|\mu|$ increases with pH. This is because that the lower the pH, the higher the concentration of H^+, and its shielding effect leads to a smaller net amount of negative fixed charges in the membrane phase. Also, the lower the pH, the less the degree of dissociation of HA, and therefore, the smaller the $|\mu|$.

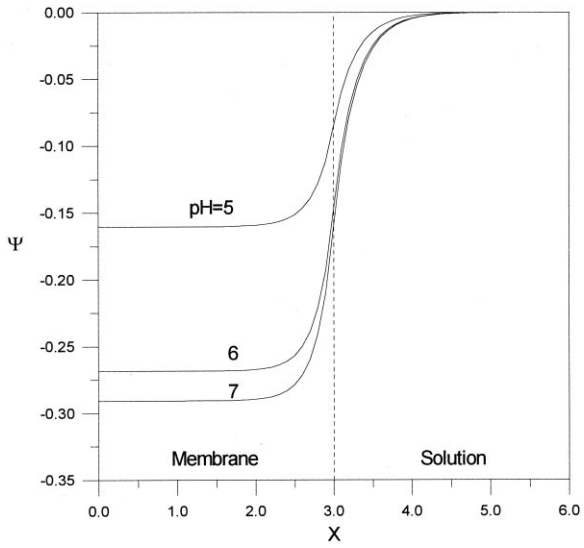

Fig. 4. Spatial variation of the scaled electrical potential ψ at various pH values for the case $\varepsilon' = 1$, $K_e = 10^{-5}$ M, $C_a^0 = 0.01$ M, $C_H^0 = 10^{-7}$ M, $N_0 = 0.05$ M, $T = 298.15$ K, $a = 3$ and $b = 1$.

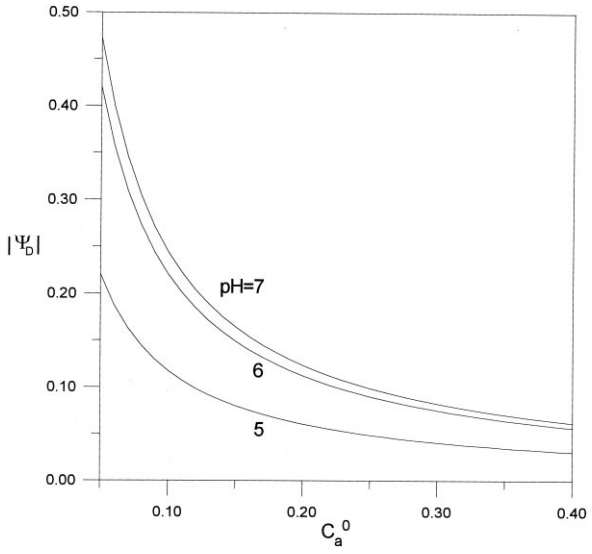

Fig. 3. Variation in the absolute scaled Donnan potential $|\psi_D|$ as a function of the concentration of cation at various pH values for the case $a = b = 1$. Key: same as Fig. 2.

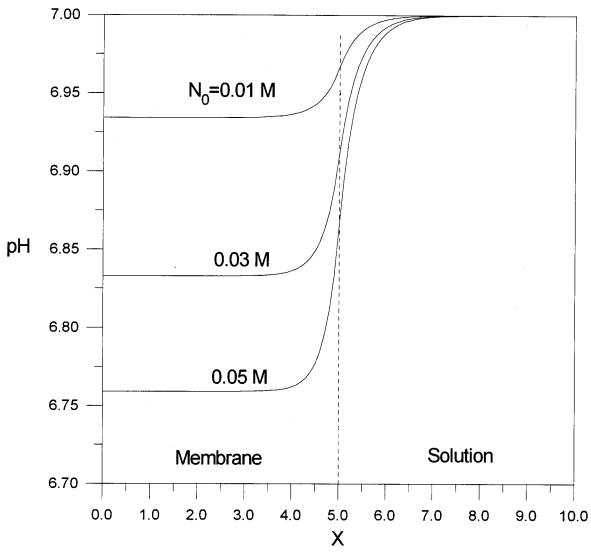

Fig. 5. Spatial variation in pH at various concentrations of functional groups for the case $d' = 5$, $C_a^0 = 0.01$ M, $a = 2$ and $b = 1$. Key: same as Fig. 2.

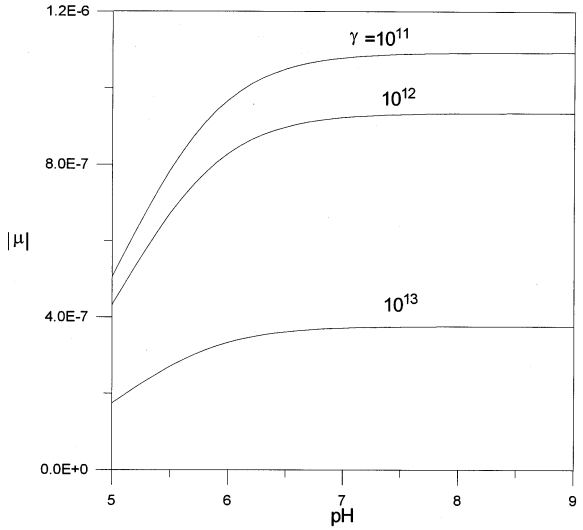

Fig. 6. Variation in the absolute mobility $|\mu|$ as a function of pH at various values of friction coefficient γ for the case $d' = 5$, $C_a^0 = 0.01$ M, $N_0 = 0.05$ M, $a = 3$ and $b = 1$. Key: same as Fig. 2.

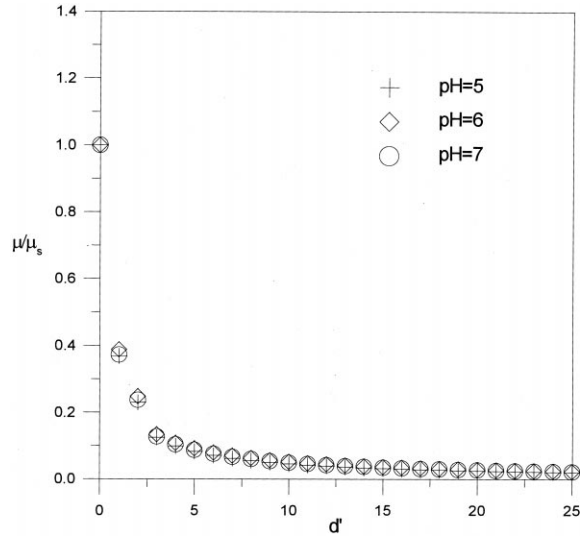

Fig. 7. Variation in the ratio μ/μ_s as a function of the scaled thickness of membrane at various pH values for the case the total number of dissociable functional groups in membrane is fixed. Parameters used are $N_0 d' = 0.2$ M, $C_a^0 = 0.01$ M, $\gamma = 10^{16}$, $a = 3$ and $b = 1$. Key: same as Fig. 2.

Figs. 7–9 simulate the variations of the ratio μ/μ_s (= mobility of a cell/mobility of a rigid particle), as a function of the scaled thickness of membrane d' at various γ and pH values. The total number of dissociable functional groups is fixed. Note that if $d' = 0$, the mobility reduces to that predicted by the Smoluchowski's theory for a rigid particle, Eq. (1), and $\mu/\mu_s = 1$. Fig. 7 suggests that if γ is large, μ/μ_s is less than unity, and it decreases with the increase in d', and μ/μ_s is insensitive to the variation in pH. On the other hand, if γ is small, μ/μ_s increases with d', and μ/μ_s increases with pH, as can be seen from Fig. 8. It is interesting to note that for a medium γ, the variation of μ/μ_s as a function of d' has a local maximum, as illustrated in Fig. 9. This can be elaborated as follows. The greater the d', the easier for the functional group in the membrane phase to dissociate, and the greater the amount the fixed charges. On the other hand, the total resistance due to the presence of the membrane phase also increases with d'. If d' is small, the former effect dominates, and μ/μ_s increases with d', and the reverse is true if d' is large. Therefore, a local maximum for μ/μ_s may exist at a medium d'. Note that, depending upon the thickness of membrane, μ/μ_s can be either greater or less than unity.

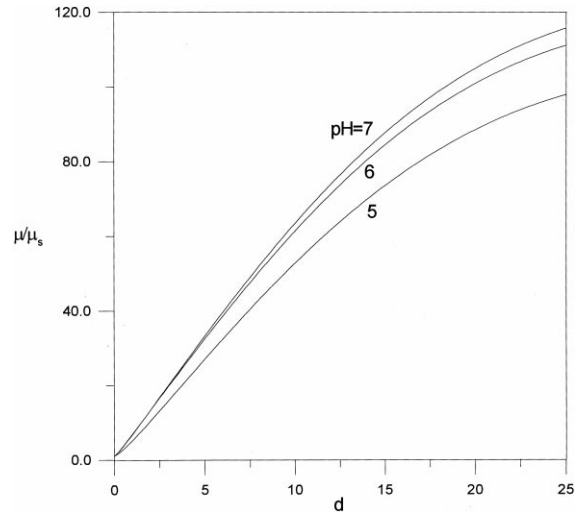

Fig. 8. Variation in the ratio μ/μ_s as a function of the scaled thickness of membrane at various pH values for the case of Fig. 7 except that $\gamma = 10^{11}$.

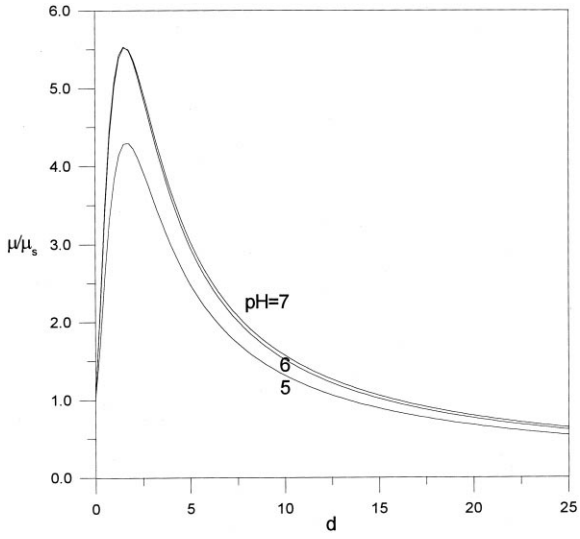

Fig. 9. Variation in the ratio μ/μ_s as a function of the scaled thickness of membrane at various pH values for the case of Fig. 7 except that $\gamma = 5 \times 10^{13}$.

The classic result for a rigid particle can be recovered as a limiting case of the present model. Suppose that the total number of functional groups in the membrane phase, $-zN_0\mathrm{d}F$, remains constant, and the thickness of membrane approaches zero, i.e., the membrane phase vanishes, and the functional groups, or the fixed charges, are distributed over a rigid surface with density σ_d. We have

$$\begin{aligned}\sigma_d &= -\varepsilon_2\left(\frac{\mathrm{d}\varphi}{\mathrm{d}X}\right)_{X=0} = -\frac{\varepsilon_2 RT\kappa_2}{F}\left(\frac{\mathrm{d}\psi}{\mathrm{d}X}\right)_{X=0} \\ &= -\frac{\varepsilon_2 RT\kappa_2}{F}\{2\{\frac{a}{b}(e^{b\psi_s}-1)+e^{-a\psi_s}-1 \\ &\quad + M_H[\frac{1}{b}(e^{b\psi_s}-1)+e^{-\psi_s}-1]\}\}^{1/2} \\ &= -\frac{F}{1+M_e e^{-\psi_s}}\lim_{\substack{N_0 d=\text{const}\\ d\to 0}}(N_0 d) \qquad (29)\end{aligned}$$

The corresponding surface potential can be determined by this expression. In this case, the mobility of the particle reduces to that described by Smoluchowski (Eq. (1)).

4. Conclusion

In summary, the electrophoretic behavior of a biological cell, simulated by a particle comprises a rigid, uncharged core with a charge-regulated membrane is discussed. A semi-analytical method, which is applicable to a general electrolyte solution, is proposed for the resolution of the governing equations of the system under consideration. The result of numerical simulation reveals that the electrophoretic mobility of the particle is influenced by the pH of the liquid phase, the concentration of charged groups contained in membrane phase, and the friction coefficient of the membrane phase. The variation of the mobility of a particle as a function of membrane width may exhibit a local maximum.

Acknowledgements

This work is supported by the National Science Council of the Republic of China.

References

[1] R.J. Hunter, Foundations of Colloid Science, vol. 1, Oxford University Press, Oxford, 1989.
[2] E. Donath, V. Pastushenko, Bioelectrochem. Bioenerg. 6 (1979) 543–554.
[3] R.W. Wunderlich, J. Colloid Interface Sci. 88 (1982) 385–397.
[4] S. Levine, M. Levine, K.A. Sharp, D.E. Brooks, Biophys. J. 42 (1983) 127–135.
[5] K.A. Sharp, D.E. Brooks, Biophys. J. 47 (1985) 563–566.
[6] G.V. Seaman, in: D.M. Sergenor (Ed.), The red blood cells, vol. 2, Academic Press, New York, 1975, pp. 1136–1229.
[7] S. Kawahata, H. Ohshima, N. Muramatus, T. Kondo, J. Colloid Interface Sci. 138 (1990) 182–186.
[8] H. Ohshima, T. Kondo, J. Colloid Interface Sci. 130 (1989) 281–282.
[9] H. Ohshima, J. Colloid Interface Sci. 163 (1994) 474–483.
[10] H. Ohshima, T. Kondo, J. Colloid Interface Sci. 116 (1987) 305–311.
[11] H. Ohshima, M. Nakamura, T. Kondo, Colloid Polym. Sci. 270 (1992) 873–877.
[12] J.P. Hsu, W.C. Hsu, Y.I. Chang, J. Colloid Interface Sci. 155 (1993) 1–8.
[13] H. Ohshima, T. Kondo, Biophys. Chem. 39 (1991) 191–198.

[14] J.P. Hsu, W.C. Hsu, Y.I. Chang, Colloid Polym. Sci. 272 (1994) 251–261.
[15] J.P. Hsu, Y.P. Fan, J. Colloid Interface Sci. 172 (1995) 230–241.
[16] J.P. Hsu, S.H. Lin, S. Tseng, J. Theor. Biol. 182 (1996) 137–145.
[17] H. Ohshima, S. Ohki, Biophys. J. 47 (1985) 673–678.